

3

Interactions and diagrammatic techniques

Unfortunately it is not possible to carry out the functional integration in closed form when the Lagrangian contains terms that are more than quadratic in the fields. The reader is invited to verify this. Thus, it is important to develop approximation techniques. An approximation that is expected to be useful when the interactions are weak is found by expanding the partition function in powers of the interaction. The convergence properties of these perturbation expansions have not been established with any degree of mathematical rigor, however. An alternative approach is to evaluate the partition function containing a given Lagrangian on a spacetime lattice using numerical Monte Carlo methods. This approach is described in Chapter 10.

3.1 Perturbation expansion

Consider a single scalar field ϕ . Other, more physical, theories such as QED, QCD, the Glashow–Weinberg–Salam model, and effective nuclear models will be considered in later chapters. The reader must be prepared now to learn some basic techniques before tackling more complicated but physically relevant theories.

The partition function is

$$Z = N' \int [d\phi] e^S \tag{3.1}$$

The action can be decomposed as

$$S = S_0 + S_1 \tag{3.2}$$

where S_0 is at most quadratic in the field and S_1 , the part due to interactions, is of higher order. We may expand (3.1) in a power series in

the part due to interaction, S_I :

$$Z = N' \int [d\phi] e^{S_0} \sum_{l=0}^{\infty} \frac{1}{l!} S_I^l \quad (3.3)$$

Taking the logarithm on both sides we get

$$\begin{aligned} \ln Z &= \ln \left(N' \int [d\phi] e^{S_0} \right) + \ln \left(1 + \sum_{l=1}^{\infty} \frac{1}{l!} \frac{\int [d\phi] e^{S_0} S_I^l}{\int [d\phi] e^{S_0}} \right) \\ &= \ln Z_0 + \ln Z_I \end{aligned} \quad (3.4)$$

This explicitly separates the interaction contributions from the ideal gas contribution, which we have evaluated already. The relevant quantity that we actually need to compute is

$$\langle S_I^l \rangle_0 = \frac{\int [d\phi] e^{S_0} S_I^l}{\int [d\phi] e^{S_0}} \quad (3.5)$$

which is the value of S_I raised to an arbitrary positive integral power and averaged over the unperturbed ensemble, represented by S_0 . The normalization of the functional integration is now irrelevant, as it cancels in the expression (3.5).

3.2 Diagrammatic rules for $\lambda\phi^4$ theory

The task of actually evaluating (3.4) and (3.5) is significantly more difficult than our compact notation would suggest. It is in fact useful to associate diagrams with the mathematical expressions in the expansion. Diagrams are a common language in particle physics, nuclear physics, statistical physics and condensed matter physics and allow for the exchange of ideas and concepts among these different disciplines.

Consider the lowest-order correction to $\ln Z_0$ in $\lambda\phi^4$ theory. It is

$$\ln Z_1 = \frac{-\lambda \int d\tau \int d^3x \int [d\phi] e^{S_0} \phi^4(\mathbf{x}, \tau)}{\int [d\phi] e^{S_0}} \quad (3.6)$$

If we express $\phi(\mathbf{x}, \tau)$ as a Fourier series as in (2.30), and insert this into (3.6) we get

$$\begin{aligned} \ln Z_1 &= -\lambda \int d\tau \int d^3x \sum_{n_1, \dots, n_4} \sum_{\mathbf{p}_1, \dots, \mathbf{p}_4} \frac{\beta^2}{V^2} \\ &\quad \times \exp[i(\mathbf{p}_1 + \dots + \mathbf{p}_4) \cdot \mathbf{x}] \exp[i(\omega_{n_1} + \dots + \omega_{n_4})\tau] \frac{A}{B} \end{aligned} \quad (3.7)$$

where

$$A = \prod_l \prod_{\mathbf{q}} \int d\tilde{\phi}_l(\mathbf{q}) \exp\left[-\frac{1}{2}\beta^2(\omega_l^2 + \mathbf{q}^2 + m^2)\tilde{\phi}_l(\mathbf{q})\tilde{\phi}_{-l}(-\mathbf{q})\right] \\ \times \tilde{\phi}_{n_1}(\mathbf{p}_1)\tilde{\phi}_{n_2}(\mathbf{p}_2)\tilde{\phi}_{n_3}(\mathbf{p}_3)\tilde{\phi}_{n_4}(\mathbf{p}_4)$$

and

$$B = \prod_l \prod_{\mathbf{q}} \int d\tilde{\phi}_l(\mathbf{q}) \exp\left[-\frac{1}{2}\beta^2(\omega_l^2 + \mathbf{q}^2 + m^2)\tilde{\phi}_l(\mathbf{q})\tilde{\phi}_{-l}(-\mathbf{q})\right]$$

The integrations over \mathbf{x} and τ yield a factor $\beta V \delta_{n_1+\dots+n_4,0} \delta_{\mathbf{p}_1+\dots+\mathbf{p}_4,0}$. The numerator of the whole expression for $\ln Z_1$ will be zero by symmetric integration unless $n_3 = -n_1$, $\mathbf{p}_3 = -\mathbf{p}_1$ and $n_4 = -n_2$, $\mathbf{p}_4 = -\mathbf{p}_2$, or the other two permutations thereof. This will satisfy the constraints of the Kronecker deltas and the integrals will factorize. The integrals in the numerator are canceled by those in the denominator except for the two corresponding to $l = n_1$, $\mathbf{q} = \mathbf{p}_1$ and $l = n_2$, $\mathbf{q} = \mathbf{p}_2$, and the other two permutations. Using

$$\frac{\int_{-\infty}^{\infty} dx x^2 e^{-ax^2/2}}{\int_{-\infty}^{\infty} dx e^{-ax^2/2}} = \frac{1}{a} \tag{3.8}$$

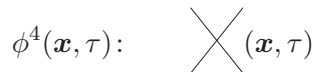
we obtain

$$\ln Z_1 = -3\lambda\beta V \left(T \sum_n \int \frac{d^3p}{(2\pi)^3} \mathcal{D}_0(\omega_n, \mathbf{p}) \right)^2 \tag{3.9}$$

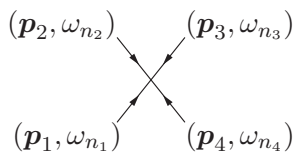
Here we have defined the propagator in frequency–momentum space as

$$\mathcal{D}_0(\omega_n, \mathbf{p}) = \frac{1}{\omega_n^2 + \mathbf{p}^2 + m^2} \tag{3.10}$$

The expression (3.9) can be associated with a diagram in the following way. Remember that we are calculating $\ln Z_1$ to first order in λ . With $\phi^4(\mathbf{x}, \tau)$ we associate a cross with four arms (because of the fourth power of ϕ), with the vertex located at (\mathbf{x}, τ) :



After expressing each field $\phi(\mathbf{x}, \tau)$ as a Fourier series we draw the figure



The directions of the arrows reflect the signs of the momenta and frequencies. By convention, we draw them pointing towards the vertex, but we could have chosen a convention in which they all point away. The functional integration vanishes unless $n_3 = -n_1$, $\mathbf{p}_3 = -\mathbf{p}_1$ and $n_4 = -n_2$, $\mathbf{p}_4 = -\mathbf{p}_2$, etc. Thus we connect the ends in pairs. There are three possible pairings. We then have

$$\ln Z_1 = 3 \begin{array}{c} \text{⦿} \\ (\mathbf{p}_1, \omega_{n_1})(\mathbf{p}_2, \omega_{n_2}) \end{array} \quad (3.11)$$

With each closed loop we associate a factor

$$T \sum_n \int \frac{d^3p}{(2\pi)^3} \mathcal{D}_0(\omega_n, \mathbf{p})$$

With the vertex we associate a factor $-\lambda$ (coming from $\mathcal{L}_I = -\lambda\phi^4$) and a factor

$$\beta\delta_{\omega_{in},\omega_{out}} V\delta_{\mathbf{p}_{in},\mathbf{p}_{out}} \rightarrow \beta\delta_{\omega_{in},\omega_{out}} (2\pi)^3\delta(\mathbf{p}_{in} - \mathbf{p}_{out})$$

Since the arguments of the frequency–momentum-conserving deltas are zero we simply get an overall factor βV . The factor V makes $\ln Z_1$ a properly extensive quantity. Pictorially, (3.11) corresponds precisely with (3.9).

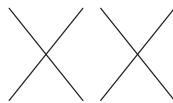
Next we look at order λ^2 in $\ln Z_1$. From (3.4) it is

$$\ln Z_2 = -\frac{1}{2} \left(\frac{\int [d\phi] e^{S_0} S_I}{\int [d\phi] e^{S_0}} \right)^2 + \frac{1}{2} \frac{\int [d\phi] e^{S_0} S_I^2}{\int [d\phi] e^{S_0}} \quad (3.12)$$

The first term in (3.12) is simply

$$-\frac{1}{2}(\ln Z_1)^2 = -\frac{1}{2} \left(3 \text{⦿} \otimes 3 \text{⦿} \right) \quad (3.13)$$

The second term in (3.12) may be analyzed algebraically using functional integrals or it may be analyzed diagrammatically. Choosing the latter approach, we draw two crosses corresponding to the factors $\phi^4(\mathbf{x}, \tau)$ and $\phi^4(\mathbf{x}', \tau')$ contained in $\frac{1}{2}\langle S_I^2 \rangle_0$:



We then pair the lines as before. Counting in the factor one-half and all the possible pairings, we obtain

$$\frac{1}{2} \times 3 \text{ (two circles)} \otimes 3 \text{ (two circles)} + \frac{6 \times 6 \times 2}{2} \text{ (three circles)} + \frac{4 \times 3 \times 2}{2} \text{ (two circles with a line between them)} \tag{3.14}$$

Combining (3.13) and (3.14), we observe that all the disconnected diagrams cancel. We are thus left with

$$\ln Z_2 = 36 \text{ (three circles)} + 12 \text{ (two circles with a line between them)} \tag{3.15}$$

What is needed at some arbitrary order N in the perturbative expansion of $\ln Z_I$ should now be clear. We formally expand in powers of λ :

$$\ln Z_I = \sum_{N=1}^{\infty} \ln Z_N \tag{3.16}$$

where $\ln Z_N$ is proportional to λ^N . The “finite-temperature Feynman rules” at order N are:

- 1 Draw all connected diagrams.
- 2 Determine the combinatoric factor for each diagram.
- 3 Include a factor $T \sum_n \int [d^3p/(2\pi)^3] \mathcal{D}_0(\omega_n, \mathbf{p})$ for each line.
- 4 Include a factor $-\lambda$ for each vertex.
- 5 Include a factor $(2\pi)^3 \delta(\mathbf{p}_{\text{in}} - \mathbf{p}_{\text{out}}) \beta \delta_{\omega_{\text{in}}, \omega_{\text{out}}}$ for each vertex, corresponding to energy(frequency)–momentum conservation. There will be one factor $\beta(2\pi)^3 \delta(\mathbf{0}) = \beta V$ left over.

We now understand why \mathcal{D} is called a propagator: it propagates a particle (or field) from one vertex to the next. We have illustrated the cancellation mechanism only at second order. However, it is clear why disconnected diagrams cancel. If, at some order, there existed a contribution that was the product of K connected diagrams then this contribution would be proportional to V^K . If we have done our job correctly, then $\ln Z_I$ is an extensive quantity proportional to V and thus no such contribution can arise.

The formal proof that in $\ln Z_I$ the disconnected diagrams cancel goes as follows. From (3.3) and (3.5) we have

$$Z_I = \sum_{l=0}^{\infty} \frac{1}{l!} \langle S_I^l \rangle_0 \tag{3.17}$$

In general, $\langle S_I^l \rangle_0$ can be written as a sum of terms, each of which is a product of connected parts (see (3.14)). Denoting a connected part by a

subscript c , we may write

$$\langle S_I^l \rangle_0 = \sum_{a_1, a_2, \dots = 0}^{\infty} \frac{l!}{a_1! a_2! (2!)^{a_2} a_3! (3!)^{a_3} \dots} \langle S_I \rangle_{0c}^{a_1} \langle S_I^2 \rangle_{0c}^{a_2} \dots \delta_{a_1 + 2a_2 + 3a_3 + \dots, l} \tag{3.18}$$

The combinatoric factor takes into account indistinguishability, and the Kronecker delta picks out the contribution of order λ^l . Substituting (3.18) into (3.17) and summing over l eliminates the Kronecker delta:

$$Z_I = \sum_{a_1, a_2, \dots = 0}^{\infty} \frac{\langle S_I \rangle_{0c}^{a_1}}{a_1!} \frac{\langle S_I^2 \rangle_{0c}^{a_2}}{a_2! (2!)^{a_2}} \dots = \exp \left(\sum_{n=1}^{\infty} \frac{1}{n!} \langle S_I^n \rangle_{0c} \right) \tag{3.19}$$

Hence $\ln Z_I$ is simply the sum of the connected diagrams.

As an example, let us apply these rules to the second diagram of (3.15). We get

$$\begin{aligned} \text{Diagram} &= \beta V (-\lambda^2) T \sum_{n_1} \int \frac{d^3 p_1}{(2\pi)^3} \dots T \sum_{n_4} \int \frac{d^3 p_4}{(2\pi)^3} \\ &\times \mathcal{D}_0(\omega_{n_1}, \mathbf{p}_1) \dots \mathcal{D}_0(\omega_{n_4}, \mathbf{p}_4) (2\pi)^3 \delta(\mathbf{p}_1 + \dots + \mathbf{p}_4) \beta \delta_{n_1 + \dots + n_4, 0} \end{aligned} \tag{3.20}$$

The evaluation of expressions such as (3.20) is not simple and will be discussed in detail in Section 3.4. The diagrammatic technique is a convenient means for keeping track of the combinatoric factors and the order of the coupling constant in a perturbative expansion of the partition function. It circumvents much of the tedious algebra associated with the direct evaluation of functional integrals.

3.3 Propagators

We shall define a finite-temperature propagator in position space by

$$\mathcal{D}(\mathbf{x}_1, \tau_1; \mathbf{x}_2, \tau_2) = \langle \phi(\mathbf{x}_1, \tau_1) \phi(\mathbf{x}_2, \tau_2) \rangle \tag{3.21}$$

where the angle brackets denote an ensemble average. Owing to translation invariance, \mathcal{D} depends only on $\mathbf{x}_1 - \mathbf{x}_2$ and $\tau_1 - \tau_2$. The Fourier transform is, with $\mathbf{x}_1 = \mathbf{x}$, $\mathbf{x}_2 = 0$, $\tau_1 = \tau$, $\tau_2 = 0$,

$$\begin{aligned} \mathcal{D}(\omega_n, \mathbf{p}) &= \int_0^\beta d\tau \int d^3 x e^{-i(\mathbf{p} \cdot \mathbf{x} + \omega_n \tau)} \mathcal{D}(\mathbf{x}, \tau) \\ &= \sum_{n_1, n_2} \sum_{\mathbf{p}_1, \mathbf{p}_2} \frac{\beta}{V} \langle \tilde{\phi}_{n_1}(\mathbf{p}_1) \tilde{\phi}_{n_2}(\mathbf{p}_2) \rangle \int_0^\beta d\tau \int d^3 x \\ &\times \exp[i(\mathbf{p}_1 - \mathbf{p}) \cdot \mathbf{x}] \exp[i(\omega_{n_1} - \omega_n) \tau] \end{aligned} \tag{3.22}$$

The ensemble average vanishes by symmetric integration unless $n_1 = -n_2$, $\mathbf{p}_1 = -\mathbf{p}_2$. Then

$$\mathcal{D}(\omega_n, \mathbf{p}) = \beta^2 \langle \tilde{\phi}_n(\mathbf{p}) \tilde{\phi}_{-n}(-\mathbf{p}) \rangle \quad (3.23)$$

We remind the reader at this point of the concept of a functional derivative. Consider the integral

$$I = I[f] = \int dx f(x) w(x)$$

where $w(x)$ is some weight function and I is a functional of $f(x)$, i.e., it depends on the function $f(x)$. The functional derivative of I with respect to $f(y)$ is

$$\frac{\delta I}{\delta f(y)} = w(y)$$

The generalization to more complicated functionals of $f(x)$ is immediate.

Recalling (3.3), (2.31), and (3.10), we discover that $\mathcal{D}(\omega_n, \mathbf{p})$ can be expressed as a functional derivative of $\ln Z$ with respect to $\mathcal{D}_0(\omega_n, \mathbf{p})$. Then

$$\begin{aligned} \mathcal{D}(\omega_n, \mathbf{p}) &= \beta^2 \frac{\int [d\phi] e^S \tilde{\phi}_n(\mathbf{p}) \tilde{\phi}_{-n}(-\mathbf{p})}{\int [d\phi] e^S} \\ &= -2 \frac{\delta \ln Z}{\delta \mathcal{D}_0^{-1}} = 2\mathcal{D}_0^2 \frac{\delta \ln Z}{\delta \mathcal{D}_0} \end{aligned} \quad (3.24)$$

Unless otherwise indicated, the symbol \mathcal{D} will from now on refer to the propagator in frequency-momentum space.

We define the self-energy $\Pi(\omega_n, \mathbf{p})$ by

$$\begin{aligned} \mathcal{D}(\omega_n, \mathbf{p}) &= [\omega_n^2 + \mathbf{p}^2 + m^2 + \Pi(\omega_n, \mathbf{p})]^{-1} \\ &= (1 + \mathcal{D}_0 \Pi)^{-1} \mathcal{D}_0 \end{aligned} \quad (3.25)$$

We shall see shortly that, in the absence of interactions, $\Pi = 0$ and $\mathcal{D} = \mathcal{D}_0$, the free-particle propagator. Using (3.25) and (3.24),

$$(1 + \mathcal{D}_0 \Pi)^{-1} = 2\mathcal{D}_0 \frac{\delta \ln Z}{\delta \mathcal{D}_0} \quad (3.26)$$

Recall from (2.33) that

$$\ln Z_0 = \frac{1}{2} \sum_n \sum_{\mathbf{q}} \ln [\mathcal{D}_0(\omega_n, \mathbf{q}) \beta^{-2}] \quad (3.27)$$

Thus

$$\frac{\delta \ln Z_0}{\delta \mathcal{D}_0(\omega_n, \mathbf{p})} = \frac{1}{2} \mathcal{D}_0^{-1}(\omega_n, \mathbf{p}) \quad (3.28)$$

and so (3.26) becomes

$$(1 + \mathcal{D}_0\Pi)^{-1} = 1 + 2\mathcal{D}_0 \frac{\delta \ln Z_1}{\delta \mathcal{D}_0} \tag{3.29}$$

It is useful to consider the formal expansion of Π in a power series in λ :

$$\Pi = \sum_{l=1}^{\infty} \Pi_l \tag{3.30}$$

Here Π_l is ostensibly of order l in the coupling constant. Let us see how (3.29) works at the first few orders. Expanding to first order, we obtain

$$\begin{aligned} 1 - \mathcal{D}_0\Pi_1 &= 1 + 2\mathcal{D}_0 \frac{\delta \ln Z_1}{\delta \mathcal{D}_0} \\ &= 1 + 2\mathcal{D}_0 \frac{\delta}{\delta \mathcal{D}_0} \left(3 \text{ (figure 8)} \right) \\ &= 1 + 12\mathcal{D}_0 \text{ (circle)} \end{aligned} \tag{3.31}$$

Thus, differentiating $\ln Z_1$ with respect to \mathcal{D}_0 is equivalent to cutting each line in the diagram, as inspection of (3.9) shows. A factor 2 appears because we can choose either of the two lines in the “figure 8”. Thus

$$\Pi_1 = -12 \text{ (circle)} \tag{3.32}$$

Continuing in this way, we seek the second-order contribution to Π . Again differentiating (3.29) and keeping terms of order λ^2 , we obtain

$$\begin{aligned} -\mathcal{D}_0\Pi_2 + \mathcal{D}_0\Pi_1\mathcal{D}_0\Pi_1 &= 2\mathcal{D}_0 \frac{\delta \ln Z_2}{\delta \mathcal{D}_0} \\ &= 2\mathcal{D}_0 \frac{\delta}{\delta \mathcal{D}_0} \left(36 \text{ (three circles)} + 12 \text{ (figure 8)} \right) \\ &= 144\mathcal{D}_0 \text{ (two circles)} + 96\mathcal{D}_0 \text{ (circle with line)} \\ &\quad + 144\mathcal{D}_0 \text{ (two circles)} \end{aligned} \tag{3.33}$$

The term $\mathcal{D}_0\Pi_1\mathcal{D}_0\Pi_1$ on the left-hand side simply cancels the last diagram on the right-hand side. Thus

$$\Pi_2 = -144 \text{ (two circles)} - 96 \text{ (circle with line)} \tag{3.34}$$

The last diagram in (3.33) is one-particle reducible; that is, by cutting one line we can break the diagram into two disconnected parts. The first two

diagrams in (3.33) are not of that form, they are one-particle irreducible (1PI). It is apparent that the one-particle reducible diagrams arise from the iteration of $\mathcal{D}_0\Pi$ in the denominator of (3.29),

$$\Pi = -2 \left(\frac{\delta \ln Z_I}{\delta \mathcal{D}_0} \right)_{1PI} \tag{3.35}$$

where by 1PI we mean that only the 1PI diagrams contribute to Π . The procedure is then as follows. First draw all diagrams which contribute to $\ln Z_I$ up to a given order, then differentiate with respect to \mathcal{D}_0 , and, lastly, throw away the one-particle reducible diagrams. This yields the diagrammatic expansion of Π .

3.4 First-order corrections to Π and $\ln Z$

Let us evaluate the one-loop diagram in (3.32). It yields the expression

$$\Pi_1 = 12\lambda T \sum_n \int \frac{d^3p}{(2\pi)^3} \frac{1}{\omega_n^2 + \omega^2} \tag{3.36}$$

where $\omega^2 = \mathbf{p}^2 + m^2$. We could do the frequency sum using (2.97), but there is a more elegant method, which we sketch below.

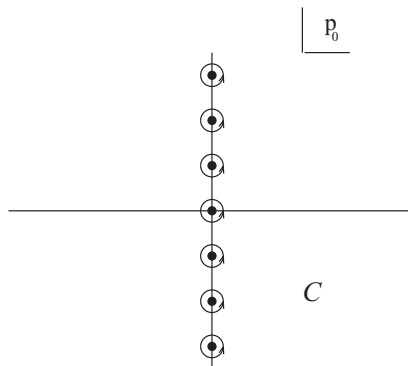
Suppose we want to evaluate a frequency sum of the form

$$T \sum_{n=-\infty}^{\infty} f(p_0 = i\omega_n = 2\pi nTi) \tag{3.37}$$

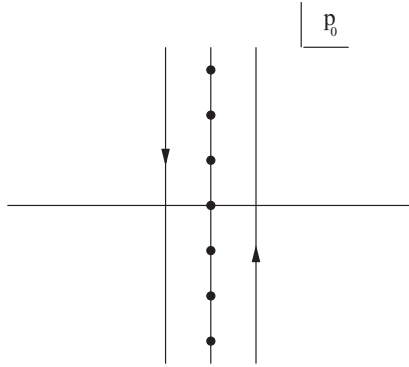
Here we think of p_0 as the fourth component of a Minkowski four-vector. We may express (3.37) as a contour integral,

$$\frac{T}{2\pi i} \oint_C dp_0 f(p_0) \frac{1}{2} \beta \coth \left(\frac{1}{2} \beta p_0 \right) \tag{3.38}$$

where the contour C is as shown in the following figure:



The function $\frac{1}{2}\beta \coth(\frac{1}{2}\beta p_0)$ has poles at $p_0 = 2\pi nTi$ and is everywhere else bounded and analytic. The contour can be deformed into



Then, with a suitable rearrangement of the exponentials in the hyperbolic cotangent, we get

$$\begin{aligned} & \frac{1}{2\pi i} \int_{i\infty-\epsilon}^{-i\infty-\epsilon} dp_0 f(p_0) \left(-\frac{1}{2} - \frac{1}{e^{-\beta p_0} - 1} \right) \\ & + \frac{1}{2\pi i} \int_{-i\infty+\epsilon}^{i\infty+\epsilon} dp_0 f(p_0) \left(\frac{1}{2} + \frac{1}{e^{\beta p_0} - 1} \right) \end{aligned} \quad (3.39)$$

Setting $p_0 \rightarrow -p_0$ in the first integral,

$$\begin{aligned} T \sum_{n=-\infty}^{\infty} f(p_0 = i\omega_n) &= \frac{1}{2\pi i} \int_{-i\infty}^{i\infty} dp_0 \frac{1}{2} [f(p_0) + f(-p_0)] \\ &+ \frac{1}{2\pi i} \int_{-i\infty+\epsilon}^{i\infty+\epsilon} dp_0 [f(p_0) + f(-p_0)] \frac{1}{e^{\beta p_0} - 1} \end{aligned} \quad (3.40)$$

This expression is correct as long as $f(p_0)$ has no singularities along the imaginary p_0 axis. The frequency sum then naturally separates into a temperature-independent part (the vacuum part) and a part containing the Bose–Einstein distribution (the matter part). In some sense, the replacement of frequency sums by contour integrals, as in (3.40), is equivalent to switching from imaginary time (discrete frequencies in Euclidean space) to real time (continuous energies in Minkowski space). However this is only a matter of mathematical convenience and involves no new physics.

Using (3.40), Π_1 can now be evaluated. With $f(p_0) = -1/(p_0^2 - \omega^2)$ we obtain

$$\Pi_1 = \Pi_1^{\text{vac}} + \Pi_1^{\text{mat}} \quad (3.41)$$

where

$$\begin{aligned}\Pi_1^{\text{vac}} &= 12\lambda \int \frac{d^4 p}{(2\pi)^4} \frac{1}{p_4^2 + \mathbf{p}^2 + m^2} \\ \Pi_1^{\text{mat}} &= 12\lambda \int \frac{d^3 p}{(2\pi)^3} \frac{1}{\omega} \frac{1}{e^{\beta\omega} - 1}\end{aligned}$$

For Π_1^{vac} we have simply defined $p_4 = ip_0$ and $d^4 p = dp_4 d^3 p$, with p_4 integrated from $-\infty$ to ∞ . This is the standard result of $T = 0$ field theory in four Euclidean dimensions. For Π_1^{mat} , we have closed the contour about the only pole in the right-hand half-plane, located at $p_0 = \omega$. There is no surface contribution since the integrand falls off sufficiently rapidly as $|p_0| \rightarrow \infty$.

The vacuum contribution to Π is actually divergent. This divergence needs to be regulated. The most straightforward way of doing this is to place a high-momentum cutoff, Λ_c , on $p \equiv \sqrt{p_4^2 + \mathbf{p}^2}$. Since the solid angle subtended by a hypersphere in n dimensions is $\Omega_n = 2\pi^{n/2}[\Gamma(n/2)]^{-1}$, we get

$$\begin{aligned}\Pi_1^{\text{vac}} &= \frac{3\lambda}{2\pi^2} \int_0^{\Lambda_c} \frac{p^3 dp}{p^2 + m^2} = \frac{3\lambda}{4\pi^2} \left[\Lambda_c^2 - m^2 \ln \left(\frac{\Lambda_c^2 + m^2}{m^2} \right) \right] \\ &\rightarrow \frac{3\lambda}{4\pi^2} \left[\Lambda_c^2 - m^2 \ln \left(\frac{\Lambda_c^2}{m^2} \right) \right]\end{aligned}\quad (3.42)$$

where the arrow indicates that terms that vanish as $\Lambda_c \rightarrow \infty$ have been dropped. At $T = 0$, the inverse propagator to first order in λ is

$$\mathcal{D}^{-1}(p_4, \mathbf{p}) = p_4^2 + \mathbf{p}^2 + m^2 + \Pi_1^{\text{vac}}\quad (3.43)$$

In order to avoid a divergent mass we add a counterterm $-\frac{1}{2}\delta m^2 \phi^2$ to the Lagrangian. Treating this as an additional interaction, we see from (3.4) and (3.5) that to lowest order this counterterm contributes to $\ln Z_1$ as

$$-\frac{1}{2}\delta m^2 \langle \phi^2 \rangle_0 = -\frac{1}{2} \text{---}\bigcirc\text{---}\quad (3.44)$$

The cross represents δm^2 . The corresponding contribution to the self-energy is, from (3.35),

$$\text{---}\times\text{---} = \delta m^2\quad (3.45)$$

Adding (3.45) to (3.42) we obtain the renormalized self-energy. We choose the counterterm so that

$$\Pi_1^{\text{vac,ren}} = \frac{3\lambda}{4\pi^2} \left[\Lambda_c^2 - m^2 \ln \left(\frac{\Lambda_c^2}{m^2} \right) \right] + \delta m^2 = 0\quad (3.46)$$

Then m remains as the physical mass of the particle. More generally, we expand δm^2 in a power series in λ :

$$\delta m^2 = \sum_{n=1}^{\infty} c_n(\Lambda_c) \lambda^n \quad (3.47)$$

and determine coefficients such that $\Pi^{\text{vac,ren}}(p^2 = M^2) = 0$ at each order in perturbation theory, at some arbitrary subtraction point M . This is part of the renormalization program, which is outside the scope of this book. The relevance of the renormalization group at finite temperature and chemical potential is discussed briefly in Chapter 4.

The complete renormalized self-energy at $T > 0$ at first order in λ is then

$$\Pi_1^{\text{ren}} = 12\lambda \int \frac{d^3p}{(2\pi)^3} \frac{1}{\omega} \frac{1}{e^{\beta\omega} - 1} \rightarrow \lambda T^2 \quad (3.48)$$

where the arrow indicates its value as $m \rightarrow 0$. Notice that Π_1^{ren} is finite and vanishes when $T = 0$. It is also momentum independent, but this is not generally true for higher-order diagrams.

Next we calculate the lowest-order correction to $\ln Z$. It is

$$\begin{aligned} 3 \text{ (two circles)} - \frac{1}{2} \text{ (circle with cross)} &= -3\lambda\beta V \left(T \sum_n \int \frac{d^3p}{(2\pi)^3} \mathcal{D}_0(\omega_n, \mathbf{p}) \right)^2 \\ &\quad - \frac{1}{2}\beta V \delta m^2 T \sum_n \int \frac{d^3p}{(2\pi)^3} \mathcal{D}_0(\omega_n, \mathbf{p}) \\ &= -3\lambda\beta V \left(\int \frac{d^3p}{(2\pi)^3} \frac{1}{\omega} \frac{1}{e^{\beta\omega} - 1} \right)^2 \\ &\quad + \frac{3\lambda\beta V}{256\pi^4} \Lambda_c^4 \left[1 - \left(\frac{m^2}{\Lambda_c^2} \right) \ln \left(\frac{\Lambda_c^2}{m^2} \right) \right]^2 \end{aligned} \quad (3.49)$$

The last term is a (divergent) contribution to the zero-point energy and pressure of the vacuum (at $T = 0$, $P = \ln Z/\beta V = -E/V$). Since only pressure and energy differences are physically measurable, this term does not contribute to the finite-temperature pressure. If we agree to normalize the vacuum pressure and energy density to zero then the physical pressure contribution at order λ is

$$P_1 = -3\lambda \left(\int \frac{d^3p}{(2\pi)^3} \frac{1}{\omega} \frac{1}{e^{\beta\omega} - 1} \right)^2 \quad (3.50)$$

When $m = 0$ and $\lambda \ll 1$ then, from (2.40) and (3.50),

$$P = T^4 \left(\frac{\pi^2}{90} - \frac{\lambda}{48} + \dots \right) \quad (3.51)$$

The pressure should be proportional to T^4 by dimensional analysis.

In these calculations, no new ultraviolet (high-momentum or short-distance) divergences appear at finite temperature. All such divergences are already present at $T = 0$; whatever regulation and renormalization is necessary at $T = 0$ is sufficient at $T > 0$ as well. This can be understood in three alternative ways. (i) We construct a complete set of states that are eigenstates of the Hamiltonian with energies E_S . In practice, for an interacting field theory this is usually impossible, but let us imagine it has been done. Then the partition function is obtained directly as

$$Z = \sum_S e^{-\beta E_S} \quad (3.52)$$

and no new $T > 0$ divergences can arise. (ii) We go back to the transition amplitude (2.16) and compute this quantity as a function of t_f . To obtain the thermodynamic partition function we simply analytically continue from real to imaginary time. (iii) We recall that in the diagrammatic expansions each internal loop involves a frequency sum. The frequency sum can be expressed as a sum of contour integrals, one corresponding to $T = 0$ and the other to $T > 0$; see (3.40). The vacuum integral can give rise to quadratic or logarithmic ultraviolet divergences. The finite-temperature integral is cut off exponentially in the ultraviolet region by the Bose–Einstein distribution. That is to say, the very-short-distance behavior of the theory is unaffected by finite temperature.

3.5 Summation of infrared divergences

The next-order contribution to $\ln Z$ when $m = 0$ is actually of order $\lambda^{3/2}$ and not λ^2 because of a finite-temperature infrared divergence in the perturbative expansion. To see this, consider the second diagram in (3.15). To study its infrared structure, let $n_1 = n_2 = n_3 = n_4 = 0$ and $\mathbf{p}_1 \sim \mathbf{p}_2 \sim \mathbf{p}_3 \sim \mathbf{p}_4 \sim \mathbf{p}$. In the limit $\mathbf{p} \rightarrow 0$ this diagram behaves like $\beta V \lambda^2 T^3 dp$, which is infrared convergent. The first diagram in (3.15) has an entirely different structure. Each of the two end loops is proportional to Π_1 . Setting $n = 0$ in the middle loop and letting \mathbf{p} denote the three-momentum flowing in that loop, we find that the behavior is $\beta V \Pi_1^2 T dp p^{-2}$. This is infrared (small- p) divergent. This divergence is unrelated to the ultraviolet divergences of the field theory at $T = 0$. This new divergence at $T > 0$, when $m = 0$, is due to the fact that $\Pi_1 \neq 0$. The boson develops a dynamically generated mass-squared, $m_{\text{eff}}^2 = \Pi_1^{\text{ren}} = \lambda T^2$. However, we

are expanding perturbatively with a propagator that has zero mass. The dynamically generated mass should then damp the infrared divergence.

At order λ^N it is easy to see that the dominant infrared divergent diagram is

$$\frac{(2 \times 3!)^N}{2N} \cdot \text{[Diagram: a circle with two external lines at each vertex]} \cdot (N \text{ loops}) \sim \beta V \Pi_1^N T dp p^{-2(N-1)} \quad (3.53)$$

The combinatoric factor arises as follows: a factor $3!$ for two connecting lines at each vertex; a factor 2 for the connection of the remaining two lines at each vertex to the adjacent vertices; a factor $(N - 1)!/2$ giving the number of ways to order the vertices in a circle; and a factor $1/N!$ coming from $S_1^N/N!$. We see that the divergence becomes more and more severe at each successive order. Because of the similarity in structure, it is possible to sum this infinite series of diagrams. Summing from $N = 2$ to ∞ we get

$$\begin{aligned} & \frac{1}{2} \beta VT \sum_n \int \frac{d^3 p}{(2\pi)^3} \sum_{N=2}^{\infty} \frac{1}{N} [-\Pi_1(\omega_n, \mathbf{p}) \mathcal{D}_0(\omega_n, \mathbf{p})]^N \\ &= \frac{1}{2} \left[\frac{1}{2} \text{[Diagram: circle with two external lines]} - \frac{1}{3} \text{[Diagram: circle with three external lines]} + \dots \right] \\ &= -\frac{1}{2} \beta VT \sum_n \int \frac{d^3 p}{(2\pi)^3} [\ln(1 + \Pi_1 \mathcal{D}_0) - \Pi_1 \mathcal{D}_0] \quad (3.54) \end{aligned}$$

This set of diagrams is sometimes called the set of ring, correlation, or plasmon diagrams in the literature (Gell-Mann and Brueckner) [1]. A more complete summation of the sub-dominant infrared divergent diagrams actually yields the full self-energy in (3.54) instead of the self-energy calculated to first order.

In obtaining (3.54) we summed only the diagrams from (3.53). In addition, there will be diagrams like (3.53) except that any number of the exterior loops are replaced by crosses corresponding to the mass counter-term δm^2 . Including those as well (this is left as an exercise), the factor Π_1 in (3.54) is replaced by $\Pi_1^{\text{ren}} = \lambda T^2$:

$$-\frac{1}{2} \beta VT \sum_n \int \frac{d^3 p}{(2\pi)^3} \left[\ln \left(1 + \frac{\lambda T^2}{\omega_n^2 + \mathbf{p}^2} \right) - \frac{\lambda T^2}{\omega_n^2 + \mathbf{p}^2} \right] = \frac{\beta V}{12\pi} \lambda^{3/2} T^4 + \dots \quad (3.55)$$

The $\lambda^{3/2}$ term arises solely from the $n = 0$ mode, which yields the dominant infrared divergence. The $n \neq 0$ modes produce higher-order corrections in λ . The origin of this nonanalyticity in λ is the fact that the boson acquires a mass proportional to $\lambda^{1/2} T$. The weak coupling expansion for

the pressure is thus

$$P = \frac{\pi^2}{90} T^4 \left[1 - \frac{15}{8} \left(\frac{\lambda}{\pi^2} \right) + \frac{15}{2} \left(\frac{\lambda}{\pi^2} \right)^{3/2} + \dots \right] \quad (3.56)$$

A nonanalyticity in the couplings of this type is also found in QED and QCD. It is good to see how this happens in a simpler theory such as $\lambda\phi^4$ first.

The same nonanalyticity should also be expected in Π because of the close relationship between Π and Z_I , as expressed in (3.35). The dominant infrared contribution at order λ^N comes from the diagram

$$\begin{aligned} & -(2 \times 3!)^N \underbrace{\text{diagram}}_{(N-1 \text{ loops})} \\ & = 12\lambda T \sum_n \int \frac{d^3p}{(2\pi)^3} [-\Pi_1(\omega_n, \mathbf{p})]^{N-1} \mathcal{D}_0^N(\omega_n, \mathbf{p}) \end{aligned} \quad (3.57)$$

Summing (3.57) from $N = 1$ to ∞ , we obtain

$$\begin{aligned} \Pi & = 12\lambda T \sum_n \int \frac{d^3p}{(2\pi)^3} \frac{1}{\omega_n^2 + \mathbf{p}^2 + \Pi_1} \\ & = -12 \underbrace{\text{diagram}}_{\mathcal{D}_1} \end{aligned} \quad (3.58)$$

which has the nice interpretation that the free propagator is replaced by the first-order-corrected propagator \mathcal{D}_1 in the one-loop self-energy diagrams. Actually, we are suppressing all other similar diagrams involving the replacement of Π_1 by δm^2 , just as in (3.54). Taking into account the mass counterterms simply replaces Π_1 by $\Pi_1 + \delta m^2 = \Pi_1^{\text{ren}}$ in (3.58). Recalling (3.41) leads to

$$\Pi_1^{\text{ren}} = \lambda T^2 \left[1 - 3 \left(\frac{\lambda}{\pi^2} \right)^{1/2} + \dots \right] \quad (3.59)$$

Thus there is a term in the self-energy of order $\lambda^{3/2}$, just as in $\ln Z_I$.

3.6 Yukawa theory

The simplest theory involving interacting fermions is one in which fermions are coupled to a neutral field by the Yukawa interaction

$$\mathcal{L}_I = g\bar{\psi}\psi\phi \quad (3.60)$$

The perturbation expansion in this case proceeds as in the previous sections with only a few changes. Since

$$S_I = \int_0^\beta d\tau \int d^3x \mathcal{L}_I(\mathbf{x}, \tau) \tag{3.61}$$

is linear in ϕ , it follows that $\langle S_I^l \rangle = 0$ if l is odd. Here the expansion of $\ln Z$ is formally an expansion in g^2 . The lowest-order correction to $\ln Z_0$ is

$$\begin{aligned} \ln Z_2 = \frac{1}{2} \langle S_I^2 \rangle_0 &= \frac{1}{2} g^2 \int d\tau_1 d\tau_2 \int d^3x_1 d^3x_2 \sum_{n_1, \dots, n_4} \sum_{l_1, l_2} \sum_{\mathbf{p}_1, \dots, \mathbf{p}_4} \sum_{\mathbf{q}_1, \mathbf{q}_2} \frac{\beta}{V^3} \\ &\times \exp[i(\mathbf{q}_1 + \mathbf{p}_3 - \mathbf{p}_1) \cdot \mathbf{x}_1] \exp[i(\mathbf{q}_2 + \mathbf{p}_4 - \mathbf{p}_2) \cdot \mathbf{x}_2] \\ &\times \exp[i(\omega_{l_1} + \omega_{n_3} - \omega_{n_1})\tau_1] \exp[i(\omega_{l_2} + \omega_{n_4} - \omega_{n_2})\tau_2] \frac{A}{B} \end{aligned} \tag{3.62}$$

where

$$\begin{aligned} A &= \prod_{\alpha, n, l} \prod_{\mathbf{p}, \mathbf{q}} \int d\tilde{\psi}_{\alpha; n}(\mathbf{p}) d\tilde{\psi}_{\alpha; n}(\mathbf{p}) d\tilde{\phi}_l(\mathbf{q}) \\ &\times e^{S_0} \tilde{\psi}_{\rho; n_1}(\mathbf{p}_1) \tilde{\psi}_{\rho; n_3}(\mathbf{p}_3) \tilde{\psi}_{\gamma; n_2}(\mathbf{p}_2) \tilde{\psi}_{\gamma; n_4}(\mathbf{p}_4) \tilde{\phi}_{l_1}(\mathbf{q}_1) \tilde{\phi}_{l_2}(\mathbf{q}_2) \end{aligned}$$

and

$$B = \prod_{\alpha, n, l} \prod_{\mathbf{p}, \mathbf{q}} \int d\tilde{\psi}_{\alpha; n}(\mathbf{p}) d\tilde{\psi}_{\alpha; n}(\mathbf{p}) d\tilde{\phi}_l(\mathbf{q}) e^{S_0}$$

Furthermore,

$$\begin{aligned} S_0 &= \beta \sum_n \sum_{\mathbf{p}} \tilde{\psi}_{\alpha; n}(\mathbf{p}) \mathcal{G}_0^{-1}(\omega_n, \mathbf{p})_{\alpha\rho} \tilde{\psi}_{\rho; n}(\mathbf{p}) \\ &\quad - \frac{1}{2} \beta^2 \sum_n \sum_{\mathbf{p}} \tilde{\phi}_n(\mathbf{p}) \mathcal{D}_0^{-1}(\omega_n, \mathbf{p}) \tilde{\phi}_{-n}(-\mathbf{p}) \end{aligned} \tag{3.63}$$

The free-particle fermion propagator \mathcal{G}_0 is defined, in analogy to the free-particle boson propagator, as

$$\mathcal{G}_0^{-1}(\omega_n, \mathbf{p}) = \not{p} - M \tag{3.64}$$

Here $p_0 \equiv i\omega_n + \mu$, M is the fermion mass, and m is the boson mass (see (2.91)). We have changed our variable of integration from $i\psi^\dagger$ to $\tilde{\psi}$, which is conventional.

The integration over the spatial and temporal coordinates in (3.62) can be done immediately. It leads to an overall factor of $\beta^2 V^2$ and to the constraints

$$\mathbf{p}_1 = \mathbf{p}_3 + \mathbf{q}_1 \quad \mathbf{p}_2 = \mathbf{p}_4 + \mathbf{q}_2 \quad n_1 = n_3 + l_1 \quad n_2 = n_4 + l_2 \tag{3.65}$$

The integration over the scalar field leads to the constraints

$$\mathbf{q}_2 = -\mathbf{q}_1 \quad l_2 = -l_1 \tag{3.66}$$

The integration over the spinor field leads to either of the following constraints:

$$\mathbf{p}_1 = \mathbf{p}_3 \quad \mathbf{p}_2 = \mathbf{p}_4 \quad n_1 = n_3 \quad n_2 = n_4$$

or

$$\mathbf{p}_1 = \mathbf{p}_4 \quad \mathbf{p}_2 = \mathbf{p}_3 \quad n_1 = n_4 \quad n_2 = n_3 \tag{3.67}$$

These two possibilities lead to two topologically distinct diagrams:

$$\ln Z_2 = \frac{1}{2} \left(\text{Diagram 1} \right) - \frac{1}{2} \left(\text{Diagram 2} \right) \tag{3.68}$$

The first of these represents

$$\frac{1}{2} \beta V \frac{g^2}{m^2} \left(T \sum_n \int \frac{d^3 p}{(2\pi)^3} \text{Tr} \mathcal{G}_0(\omega_n, \mathbf{p}) \right)^2 \tag{3.69}$$

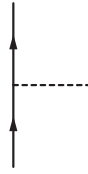
and the second represents

$$-\frac{1}{2} \beta V g^2 T^2 \sum_{n_1 n_2} \int \frac{d^3 p_1 d^3 p_2}{(2\pi)^6} \times \text{Tr}[\mathcal{G}_0(\omega_{n_1}, \mathbf{p}_1) \mathcal{D}_0(\omega_{n_2} - \omega_{n_1}, \mathbf{p}_2 - \mathbf{p}_1) \mathcal{G}_0(\omega_{n_2}, \mathbf{p}_2)] \tag{3.70}$$

The solid lines represent fermions and the broken lines represent bosons. The arrows on the fermion lines indicate the flow of fermion number and follow from the fact that in (3.62) a $\bar{\psi}$ must always be matched to a ψ to get a nonzero contribution. The trace operation in (3.69) and (3.70) is over the Dirac indices. The minus sign in (3.70) comes from anticommuting the fermion fields (which are Grassmann variables) to put them into the canonical ordering of (2.80) and (2.81). The boson line in the first diagram carries zero frequency and momentum and gives rise to the factor $\mathcal{D}_0(0, \mathbf{0}) = m^{-2}$. The reader is encouraged to verify that indeed (3.68)–(3.70) follow directly from the functional integral of (3.62).

The “finite-temperature Feynman rules” are similar to those listed in Section 3.2. The new aspects are:

- 1 There is a factor $T \sum_n \int [d^3 p / (2\pi)^3] \mathcal{G}_0(\omega_n, \mathbf{p})$ for each fermion line.
- 2 There is a factor g at each vertex.
- 3 There is a trace over Dirac indices for each closed fermion loop as well as a minus sign coming from the Grassmann nature of the fermion field.
- 4 All connected diagrams are constructed from the following elementary vertex:

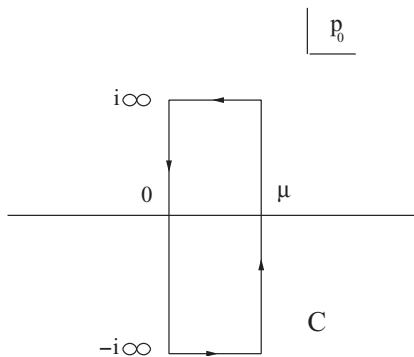


It turns out that the one-particle reducible diagrams (one of which is seen in (3.68)) arise from the fact that the scalar field ϕ develops a nonzero thermal average. It is in some sense analogous to a Bose–Einstein condensate. This condensate is however driven by the interaction with the fermions. All such diagrams can be summed by the use of the mean field expansion. This will be illustrated in later chapters.

The frequency sum for fermions can be converted to contour integrals in a manner closely paralleling the procedure for bosons. The fermion propagator depends on the combination $p_0 = i\omega_n + \mu$ with $\omega_n = (2n + 1)\pi T$. A straightforward analysis yields

$$\begin{aligned}
 T \sum_n f(p_0 = i\omega_n + \mu) &= -\frac{1}{2\pi i} \int_{-i\infty+\mu+\epsilon}^{i\infty+\mu+\epsilon} dp_0 f(p_0) \frac{1}{e^{\beta(p_0-\mu)} + 1} \\
 &\quad - \frac{1}{2\pi i} \int_{-i\infty+\mu-\epsilon}^{i\infty+\mu-\epsilon} dp_0 f(p_0) \frac{1}{e^{\beta(\mu-p_0)} + 1} \\
 &\quad + \frac{1}{2\pi i} \oint_C dp_0 f(p_0) + \frac{1}{2\pi i} \int_{-i\infty}^{i\infty} dp_0 f(p_0)
 \end{aligned}
 \tag{3.71}$$

The contour C is as shown in the following figure:



The first two terms in (3.71) correspond to particle and antiparticle contributions and vanish at $T = 0$. The third term is T -independent and gives the $T = 0$ finite-density contribution. The last term is the vacuum contribution.

The boson self-energy Π is still defined by (3.25) and still satisfies (3.35). From (3.68) the lowest-order diagram is

$$\Pi_2 = \text{---} \circlearrowleft \text{---} \tag{3.72}$$

The fermion self-energy Σ is defined by the equation

$$\mathcal{G}^{-1} = \mathcal{G}_0^{-1} + \Sigma = \not{p} - M + \Sigma(\omega_n, \mathbf{p}) \tag{3.73}$$

In position space, the full fermion propagator is defined by

$$\mathcal{G}(\mathbf{x}_1 - \mathbf{x}_2, \tau_1 - \tau_2) = \langle T_\tau [\bar{\psi}(\mathbf{x}_1, \tau_1)\psi(\mathbf{x}_2, \tau_2)] \rangle \tag{3.74}$$

where the angle brackets denote the exact ensemble average. It can be shown that the analog of (3.35) is

$$\Sigma = \frac{\delta \ln Z_I}{\delta \mathcal{G}_0} \tag{3.75}$$

From (3.68) the lowest-order diagrams are

$$\Sigma_2(\omega_n, \mathbf{p}) = \text{---} \overset{\circlearrowleft}{\text{---}} \text{---} - \text{---} \overset{\text{---}}{\text{---}} \text{---} \tag{3.76}$$

Explicit evaluations of loop diagrams involving fermions will be taken up in the later chapters on theories that represent nature.

3.7 Remarks on real time perturbation theory

The perturbative treatment discussed up to now has been in the so-called imaginary time formalism. The functional integral representation of the partition function involves an integration over “imaginary time” from 0 to β . A Fourier decomposition of the fields leads to a discrete frequency sum; for bosons $\omega_n = 2\pi nT$ and for fermions $\omega_n = (2n + 1)\pi T$.

The one-loop expression in (3.41) can be written alternatively as

$$\Pi_1 = 12\lambda \int_{-\infty}^{\infty} \frac{d^3p}{(2\pi)^3} \int_{-\infty}^{\infty} \frac{dp_0}{2\pi} \left(\frac{i}{p^2 - m^2 + i\epsilon} + \frac{2\pi}{e^{\beta|p_0|} - 1} \delta(p^2 - m^2) \right) \tag{3.77}$$

This has the interpretation that the propagator consists of the sum of a vacuum part and a finite-temperature part. Instead of a summation over discrete frequencies there is an integration over a real, continuous, energy p_0 . Because of the presence of the Dirac delta function, the finite-temperature contribution is trivial to obtain.

The above suggests the possibility of a “real time” perturbation theory. The rules of Section 3.2 could perhaps be modified according to

$$\begin{aligned}
 T \sum_n &\rightarrow \int_{-\infty}^{\infty} \frac{dp_0}{2\pi} \\
 \frac{1}{\omega_n^2 + \omega^2} &\rightarrow \frac{i}{p^2 - m^2 + i\epsilon} + \frac{2\pi}{e^{\beta|p_0|} - 1} \delta(p^2 - m^2) \\
 \beta \delta_{\omega_{\text{in}}, \omega_{\text{out}}} &\rightarrow 2\pi \delta(p_{\text{in}}^0 - p_{\text{out}}^0)
 \end{aligned} \tag{3.78}$$

The advantage would be that no frequency sums need to be done. The finite-temperature contributions are naturally separated. In addition, the Green’s functions so obtained are functions of real Minkowski momenta p^μ , which facilitates certain applications such as linear response analyses, discussed in Chapter 6.

Unfortunately, there are cases where the simple substitution (3.78) does not work [2]. As an example, consider a massive boson field with a cubic self-interaction. The one-loop self-energy diagram is

$$\Pi(k) = \frac{\text{---}\bigcirc\text{---}}{k} \tag{3.79}$$

The (unrenormalized) self-energy evaluated at zero four-momentum ($k = 0$) is

$$T \sum_n \int \frac{d^3p}{(2\pi)^3} \frac{1}{(\omega_n^2 + \omega^2)^2} \tag{3.80}$$

This expression is logarithmically divergent in the ultraviolet regime ($|p| \rightarrow \infty$), but this divergence is regulated by the usual $T = 0$ counterterm; no new $T > 0$ divergences appear. If we perform the substitution (3.78) we obtain

$$\int_{-\infty}^{\infty} \frac{dp_0}{2\pi} \int \frac{d^3p}{(2\pi)^3} \left(\frac{i}{p^2 - m^2 + i\epsilon} + \frac{2\pi}{e^{\beta|p_0|} - 1} \delta(p^2 - m^2) \right)^2 \tag{3.81}$$

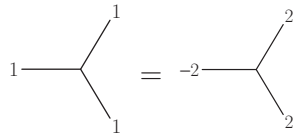
There is now a severe mathematical singularity owing to the square of the delta function. The expression (3.81) is ill-defined.

It is possible to formulate a real time perturbation theory reminiscent of (3.78) [3, 4]. Essentially, the number of independent fields doubles. Instead of a single scalar field ϕ , we encounter two scalar fields, ϕ_1 and ϕ_2 , called type-1 and type-2 fields. The propagator becomes a 2×2 matrix even

though the bosons are neutral and have no spin. The propagator is

$$\begin{aligned}
 D &= \begin{pmatrix} \cosh \theta & \sinh \theta \\ \sinh \theta & \cosh \theta \end{pmatrix} \begin{pmatrix} \frac{i}{p^2 - m^2 + i\epsilon} & 0 \\ 0 & \frac{-i}{p^2 - m^2 - i\epsilon} \end{pmatrix} \begin{pmatrix} \cosh \theta & \sinh \theta \\ \sinh \theta & \cosh \theta \end{pmatrix} \\
 &= \begin{pmatrix} \frac{i}{p^2 - m^2 + i\epsilon} & 0 \\ 0 & \frac{-i}{p^2 - m^2 - i\epsilon} \end{pmatrix} \\
 &\quad + \frac{2\pi}{e^{\beta|p_0|} - 1} \delta(p^2 - m^2) \begin{pmatrix} 1 & -e^{\beta|p_0|/2} \\ -e^{\beta|p_0|/2} & 1 \end{pmatrix} \tag{3.82}
 \end{aligned}$$

There are two types of vertex. A type-1 vertex has only type-1 fields emerging from it and has its usual value, while a type-2 vertex has only type-2 fields emerging from it and has a value opposite in sign to its type-1 counterpart. For example, for a cubic coupling,



The ultimate reason for this field doubling is to avoid singularities of the type that arise in (3.81). Explicit calculations show the cancellation arising from the two components. In this regard, the delta function appearing in (3.82) is represented as

$$\delta(p^2 - m^2) = \lim_{\epsilon \rightarrow 0} \frac{1}{\pi} \frac{\epsilon}{(p^2 - m^2)^2 + \epsilon^2} \tag{3.83}$$

Similar field doublings appear for spin-1/2 fermions and for spin-1 vector bosons.

It is interesting that perturbation theory at finite temperature can be formulated directly in real time as well as in imaginary time. Our preference is for the imaginary time formalism and this is the one adopted in this book.

3.8 Exercises

- 3.1 Derive the diagrammatic rules for the neutral scalar field with a cubic self-interaction $g\phi^3$ in $5 + 1$ dimensions. Derive the lowest-order diagrams for $\ln Z_I$ and Π .
- 3.2 Derive (3.35) to all orders.

- 3.3 Show that $\frac{1}{2}\beta \coth(\frac{1}{2}\beta p_0)$ has simple poles at $p_0 = 2\pi nTi$ with residue 1 and is elsewhere analytic and bounded.
- 3.4 Show that Π_1 is replaced by $\Pi_1^{\text{ren}} = \Pi_1 + \delta m^2$ in (3.54) when the corresponding diagrams with counterterms are included.
- 3.5 Show that (3.59) follows from (3.41) when $\lambda \ll 1$.
- 3.6 Prove (3.71).
- 3.7 Prove (3.75).

References

1. Gell-Mann, M., and Brueckner, K. A., *Phys. Rev.* **106**, 364 (1957).
2. Dolan, L., and Jackiw, R., *Phys. Rev D* **9**, 3320 (1974).
3. Umezawa, H., Matsumoto, H., and Tachiki, M. (1982). *Thermo Field Dynamics and Condensed States* (North-Holland, Amsterdam).
4. Niemi, A. J. and Semenoff, G. W., *Ann. Phys.* **152**, 105 (1984); *Nucl. Phys.* **B230**, 181 (1984).

Bibliography

Classic papers

- Dolan, L., and Jackiw, R., *Phys. Rev. D* **9**, 3320 (1974).
 Weinberg, S., *Phys. Rev. D* **9**, 3357 (1974).
 Norton, R. E. and Cornwall, J. M., *Ann. Phys.* **91**, 106 (1975).
 Lindé, A., *Rep. Prog. Phys.* **42**, 389 (1979).

Real time perturbation theory

- Umezawa, H., Matsumoto, H., and Tachiki, M. (1982). *Thermo Field Dynamics and Condensed States* (North-Holland, Amsterdam).
 Niemi, A. J. and Semenoff, G. W., *Ann. Phys.* **152**, 105 (1984); *Nucl. Phys.* **B230**, 181 (1984).
 Landsman, N. P. and van Weert, Ch. G., *Phys Rep.* **145**, 141 (1987).

Ring diagram contribution

- Gell-Mann, M., and Brueckner, K. A., *Phys. Rev.* **106**, 364 (1957).